PHYSICAL REVIEW B **68**, 201301(R) (2003)

Complex dynamics of the Si(111)-7×7 surface: Total-energy calculations

Lei Liu, C. S. Jayanthi, and Shi-Yu Wu
Department of Physics, University of Louisville, Louisville, Kentucky 40292, USA
(Received 18 June 2003; revised manuscript received 15 August 2003; published 10 November 2003)

We studied the dynamics of a semi-infinite Si(111)-7×7 system, using the force-constant matrix obtained from the total-energy calculation based on a nonorthogonal tight-binding Hamiltonian. We modeled the semi-infinite system by merging the optimized surface slab seamlessly onto the bulk to underscore the importance of the system size in obtaining all the relevant surface phonon modes of Si(111)-7×7. Our study has uncovered modes that have hitherto not been reported by *ab initio* molecular-dynamics studies and, also, provides detailed explanations of the nature of all important surface dynamical features (e.g., modes associated with dimers, adatoms, stacking faults, and rest atoms), using an analysis of the site density of states and pair density of states that identifies directly coupled vibrations.

DOI: 10.1103/PhysRevB.68.201301 PACS number(s): 68.35.Ja, 68.35.Bs, 71.15.Nc

The 7×7 dimer-adatom-stacking-fault (DAS)-reconstructed (111) surface of silicon is one of the most complicated surface systems (Fig. 1). The intricacies of this reconstructed surface structure render the study of its surface dynamics challenging as well as rewarding. Experimentally, an electron energy-loss spectroscopy (EELS) measurement[1] of the clean 7×7 surface revealed dynamical features at 25–33 meV and 71 meV. A high-resolution helium atom scattering study of the low-energy surface modes showed that Rayleigh waves (RW's) peaked at 8 meV, 10 meV, and 15 meV.[2] Theoretically, surface vibrations of the DAS model of Si(111)-7×7 have been studied via an *ab initio* cluster calculation,[1] empirical potentials,[3] a tight-binding (TB) Hamiltonian with the electron dynamics treated by Car-Parrinello fictitious Lagrangian,[4] and *ab initio* molecular-dynamics (MD) studies.[5,6] Both TB and *ab initio* studies using an identical supercell had reported similar surface dynamical features, suggesting that TB approaches will give results comparable to those from *ab initio* approaches provided they use similar computational frameworks.

In the present work, we have used a nonorthogonal TB (NOTB) Hamiltonian[7] to study the structure and dynamics of Si(111)-7×7. We consider a semi-infinite system, which is obtained by a seamless merger of an optimized surface slab onto the bulk. In addition to the previously reported surface phonon modes, our work predicts new modes that were not reported by previous theoretical/experimental studies. Succinct interpretations of the nature of these modes have been given based on a projection scheme for site density of states (SDOS). The newly uncovered prominent surface modes include low-energy RW's, a mode at 16 meV associated with the stacking fault, a mode at 57 meV confined within the first two layers, and a mode at 62 meV associated with dimers (close to the mode at 63 meV associated with the rest atom).

The differences in the surface dynamical features between previous MD studies and the present work can be attributed to the insufficient size of the supercell used in previous studies.[4–6] In previous studies, the structure and dynamics of a Si(111)-7×7 were determined using a slab of eight layers, where two central layers were held at bulk positions. Because of the imposed inversion symmetry, effectively only 151 atoms (adatoms plus atoms in the first three layers) were allowed to relax. Since surface dynamics is sensitive to relaxation, if the extent of relaxation is not adequately treated then the corresponding dynamical calculations may not capture all the surface phonon modes. Furthermore, the MD trajectory was followed for only 1.2 ps in the *ab initio* MD study, suggesting that the *ab initio* MD study may not have provided sufficiently accurate description of the low-energy modes.

To underscore the importance of the system size, we first determined the optimal size of the supercell for predicting the correct structure of Si(111)-7×7. Our calculation of the total energy based on the NOTB Hamiltonian,[7] which has been found to yield the energetics and the reconstruction of the clean Si (001) surface in excellent agreement with those obtained by density-functional theory (DFT) calculations as well as experimental results,[8] showed that the energy optimization using a supercell composed of ten layers plus adatoms (494 atoms), with atoms in the bottom four layers held at bulk positions to mimic the effect of the bulk and periodic boundary conditions imposed horizontally, is sufficient to en-

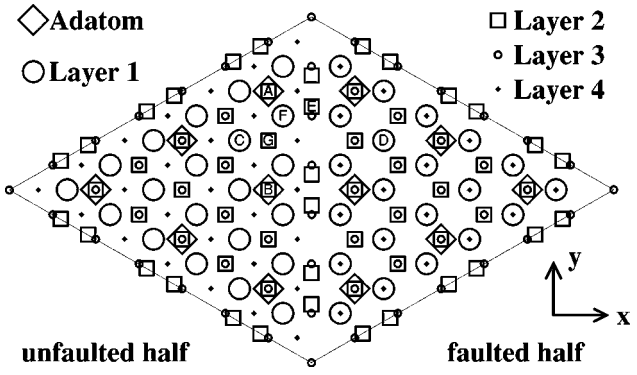

FIG. 1. A schematic top view of the DAS reconstructed Si(111)-7×7 supercell. Layer 0, 12 adatoms (6 COA's +6 CEA's); Layer 1, 42 atoms [36 capped +6 not capped by adatoms (rest atoms)]; Layer 2, 48 atoms (corner dimers, center dimers, and undimerized atoms); Layer 3, 49 atoms; etc. The faulted half has layer-4 atoms underneath the layer-1 atoms—a stacking sequence different from the unfaulted half. A combination of layer markers (L0, adatom; L1, layer 1; . . .) and position markers (A, B, . . .) will be used to specify different sites L0A, L0B, L1C, . . . , etc. in the supercell.

sure a reliable surface structural determination. Our simulation has yielded structural parameters for the Si (111) surface comparable to previous studies[4,9] with only one notable exception. We found the distance between the adatom and the atom in layer 2 directly underneath it to be about 2.97 Å, compared with a result of 2.60 Å of Ref. 4 and a result of 2.40 Å of Refs. 6,9. This substantial difference can be traced to the fact that previous studies[4,9] relaxed only adatoms and atoms in the first *three* layers (151 atoms) using a convergence criterion for the force of 0.1 $eV/$Å with only *one* layer of atoms held at bulk positions, while our optimization relaxes 298 atoms with the force criterion of 10^{-3} $eV/$Å and with four layers held at bulk positions. Thus our optimization is expected to provide a more accurate determination of the surface structure.[10] We then merged the optimized structure of the ten-layer slab onto the bulk structure to form the semi-infinite 7×7 reconstructed DAS (111) surface system.

The vibrational spectrum of this semi-infinite system was calculated layer by layer using the method of real-space Green's function.[11] In the calculation, the force-constant matrix for the adatoms and the atoms in the first six layers (298 atoms) in the semi-infinite system and the coupling force-constant matrix between atoms in the first six layers and those in layers 7–10 (interfacial layers) were computed numerically as second partial derivatives of the total energy of the original ten-layer slab about its equilibrium configuration. The force-constant matrix for the atoms in layers 7–10 and those between these atoms and atoms in subsequent bulk layers were again computed numerically as second partial derivatives of the total energy of a slab composed of layers 3–10 in the original slab plus four additional bulk layers. The bulk force-constant matrix was used as that for the remaining atoms in this semi-infinite system. In this way, the dynamical matrix of the semi-infinite system was constructed continuously and smoothly from the surface region, to the interfacial region, and to the bulk region and, thereby, treating the vibrations of all the atoms in the system on equal footing.

Figure 2 presents SDOS, as calculated from the expression $\rho_{i\alpha}(\omega)=-(2\omega/\pi)\mathrm{Im}_{\varepsilon\to0}G_{i\alpha,i\alpha}(\omega^2+i\varepsilon)$ with $G(\omega^2)=(\omega^2 I-H)^{-1}$, H being the mass-normalized force-constant matrix, I the unit matrix, i denoting the site, and α the direction, for selected adatoms, selected atoms in layers 1–4, and a bulk atom. All SDOS plots are presented on the same scale, so as to allow meaningful comparisons between them. Figure 2(a) presents the SDOS of a typical atom in the 21st layer decomposed along $x(\langle\overline{112}\rangle)$, $y(\langle\overline{110}\rangle)$, and $z(\langle111\rangle)$ directions. We have confirmed that other atoms in the 21st layer reproduce results similar to Fig. 2(a). Since the results in all the three different directions are very close to each other and in good agreement with the bulk DOS fitted to experiment,[12] we will use the SDOS shown in Fig. 2(a) to represent the SDOS for a typical atom in the bulk. A comparison of Fig. 2(a) with the SDOS for adatoms and atoms in other layers will shed light on the surface-specific features. Any deviation of SDOS along x, y, and z directions from each other may be used as a gauge of the surface effect.

Figures 2(b)–2(i) show the SDOS for strategically chosen atoms that exhibit prominent surface phonon features. The

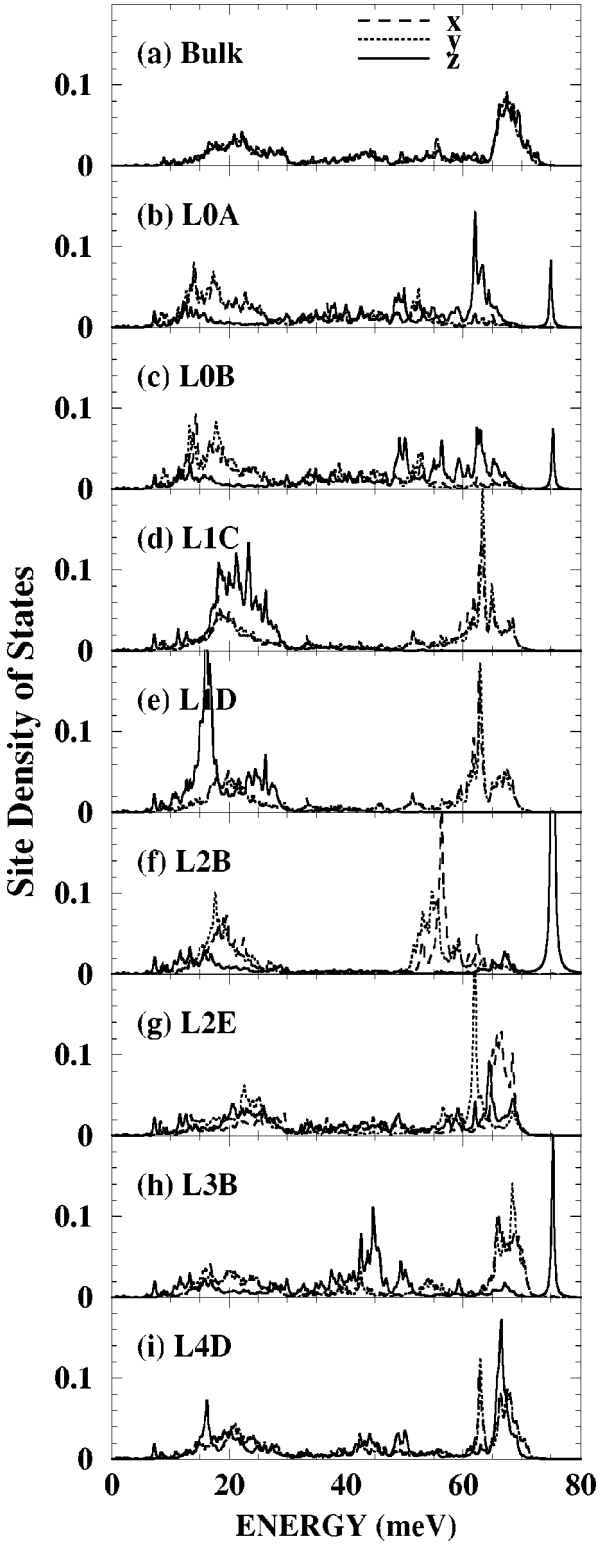

FIG. 2. SDOS for different sites in the supercell: (a) a typical bulk atom, (b) a corner adatom, (c) a center adatom, (d) a rest atom in the unfaulted half, (e) a rest atom in the faulted half, (f) a second-layer atom underneath L0B, (g) a dimer-atom, (h) a layer-3 atom directly underneath L2B, and (i) a layer-4 atom underneath L1D in the faulted half. The notations used are explained in the caption of Fig. 1.

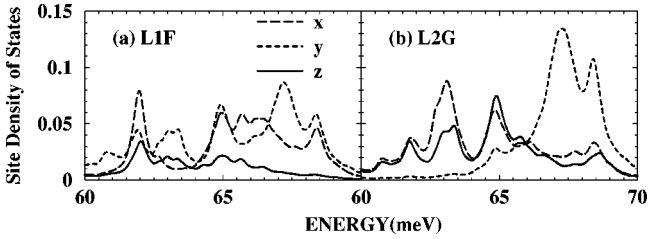

FIG. 3. SDOS of atoms at sites (a) L1F and (b) L2G. The notations used are explained in the caption of Fig. 1.

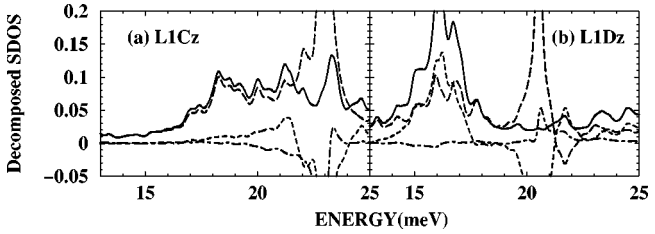

FIG. 4. SDOS for (a) ρ_{L1Cz} (solid line) and (b) ρ_{L1Dz} (solid line) in the unfaulted and faulted halves and their decomposition using Eq. (1) for $R_{ij}<3.15$ Å (long-line segment), 3.15 Å $<R_{ij}<4.15$ Å (short-line segment), and $R_{ij}>4.15$ Å (dot-dashed line) respectively.

site labels used in Fig. 2 are described in Fig. 1. Figures 2(b) and 2(c) give the SDOS for the corner adatom (COA) at L0A and the central adatom (CEA) at L0B, respectively, in the adatom layer (layer 0) of the unfaulted half. The SDOS for the atom at L0A are similar to that of atom at L0B, with both having prominent surface features at about 14 (in plane), 17 (in plane), 62 (out of plane), 63 (out of plane) and 75 meV (out of plane). We did not show SDOS for adatoms in the faulted half because they are very similar to the corresponding SDOS in the unfaulted half. In fact, the features of the SDOS for the corresponding sites in both halves are in general similar, with a few notable exceptions to be discussed later.

A comparison of SDOS, as shown in Figs. 2(c), 2(f), and 2(h) corresponding to the sites CEA-L0B, L2B (layer-2 atom directly underneath CEA-L0B), and L3B (layer-3 atom directly underneath the atom L2B), respectively, immediately identifies the split-off mode at 75 meV as a *z*-polarized mode peaked at the compressed pair of atoms L2B and L3B and attributable to the 71-meV mode observed by EELS, as also noted by previous theoretical studies.[4–6]

An examination of SDOS for COA-L0A [Fig. 2(b)] and the one for the rest atom L1C in layer 1 in the unfaulted half [Fig. 2(d)] reveals that the mode at 63 meV has its peak at the rest atom L1C, while a comparison of Figs. 2(b) and 2(g) (SDOS for atom L2E in a dimer) shows that the mode at 62 meV has its peak at the dimer. The pattern of the 63-meV mode peaked at the rest atom can be traced to the COA at L0A by examining Figs. 2(d), 3(b) (SDOS of the atom L2G that is a nearest neighbor of the rest atom L1C), 3(a) (SDOS of the atom L1F that is a nearest neighbor of both the COA at L0A and the atom L2G), and 2(b). The pronounced peak of 63-meV mode at the rest atom has almost equal *x* and *y* polarization. It then induces a vibration to its neighbor L2G polarized almost in the *xz* plane, which in turn excites its neighbor L1F to vibrate almost in *y* direction, yielding eventually an almost *z*-polarized vibration for the COA at L0A. From Figs. 2(g), 3(a), and 2(b), the pronounced peak of the 62-meV mode polarized along the dimer axis (*y* direction) of the dimer atom L2E is seen to have excited its neighbor L1F to vibrate with its polarization dominated by the *x* vibration, which in turn induces the *z*-polarized vibration for the COA at L0A. Our calculation has also shown that these three modes at 62, 63, and 75 meV are localized surface modes, with the 62 (dimer) and 75 meV (compressed atom pair) modes barely discernable at layer 4. However, the rest atom mode at 63 meV extends beyond layer 4 and exhibits different polarization in layer 4 in the faulted half [Fig. 2(i)] as compared to the unfaulted half (not shown). This can be understood as a feature associated with the stacking fault.

The effect of the stacking fault, however, shows up most prominently in the low-frequency strongly *z*-polarized mode at about 16 meV in the SDOS of the rest atom L1D in the faulted half. A comparison of Figs. 2(d) and 2(e) reveals that such a mode is not present in the SDOS of the rest atom L1C in the unfaulted half. To shed light on this unusual contrast, we decompose the SDOS in terms of the projected pair DOS (PDOS) $\overline{\rho}_{i\alpha,j\beta}$ according to $\rho_{i\alpha}(\omega)=\Sigma_{j\beta}\overline{\rho}_{i\alpha,j\beta}(\omega)$, where

$$\overline{\rho}_{i\alpha,j\beta}(\omega)=\sum_{\lambda}\frac{H_{i\alpha,j\beta}c_{i\alpha}^{\lambda}c_{j\beta}^{\lambda}(1-\delta_{ij}\delta_{\alpha\beta})}{\omega_{\lambda}^{2}-H_{i\alpha,i\alpha}}\delta(\omega-\omega_{\lambda}) \quad (1)$$

with $c_{i\alpha}^{\lambda}=\sqrt{m_i}u_{i\alpha}^{\lambda}$, $u_{i\alpha}^{\lambda}$ being the eigendisplacement of the λ mode at site i along the α direction and m_i the mass of the atom at site i.[13] It should be noted that while $\rho_{i\alpha}=\Sigma_{\lambda}(c_{i\alpha}^{\lambda})^2\delta(\omega-\omega_{\lambda})$ is always positive, individual PDOS $\overline{\rho}_{i\alpha,j\beta}(\omega)$ of Eq. (1) can be either positive or negtive, depending on the pair of atoms i and j, and the polarization of vibrations α and β. Because of the presence of $H_{i\alpha,j\beta}$, only directly coupled vibrations will contribute to the SDOS. Figure 4 gives the SDOS along the *z* axis in the vicinity of 16 meV (solid line), decomposed according to $R_{ij}\leqslant 3.15$ Å (long-line segment), 3.15 Å$<R_{ij}\leqslant 4.15$ Å (short-line segment), and 4.15 Å$<R_{ij}$ (dot-dashed line), for rest atoms in the unfaulted [Fig. 4(a)] and faulted [Fig. 4(b)] halves, respectively. Figures 4(b) and 2(i) show that the most significant contribution to the 16-meV mode peaked at the rest atom L1D in the faulted half comes from its coupled vibration with the atom L4D in layer 4 directly underneath it (distance $=3.37$ Å), with some participation of its three nearest neighbors in layer 2 and the three nearest neighbors in layer 3 of the atom at L4D. Our results also reveals that this mode is confined in the configuration composed of the eight atoms mentioned above and anchored by the out-of-phase *z* vibrations of the rest atom L1D and the layer-4 atom L4D underneath it. Since there is no such configuration in the unfaulted half as there is no atom directly underneath the rest atom L1C in layer 4, no such mode can exist for the rest atom L1C in the unfaulted half [see Fig. 4(a)]. Hence the presence and the absence of the 16-meV mode at the rest

atom L1D in the faulted and the rest atom L1C in the unfaulted half, respectively, is a direct consequence of the stacking fault.

Figures 2(f) and 2(c) show another interesting surface mode at about 57 meV. The peak of this mode is a *x*-polarized vibration at the atom L2B directly underneath the CEA at L0B in the unfaulted half and emerges as a *z*-polarized vibration of CEA at L0B, with no appreciable penetration to atoms in layer 3 and beyond. The decomposition of the SDOS along the *x* axis of atom L2B in the vicinity of 57 meV in terms of $\overline{\rho}_{L2Bx,j\beta}$ indicates that almost the entire contribution to ρ_{L2Bx} comes from its three neighboring atoms in layer 1, with no meaningful contribution from either atom L0B (directly above) or atom L3B (directly underneath). The absence of the contribution from atom L0B to the SDOS of atom L2B and the presence of the 57-meV mode as a *z*-polarized vibration in the SDOS of L0B [Fig. 2(c)] is a clear indication that the *z* vibration of atom L0B is not directly coupled to the *x* vibration of atom L2B. Thus the 57-meV mode is a mode localized within the first two layers. It involves the coupled vibrations of the *x*-polarized vibration of atom L2B with its three neighbors in layer 1 and, in turn, induces the *z*-polarized vibration of CEA at L0B.

Finally, by comparing SDOS of corresponding atoms layer by layer, we have detected the possible existence of RW's at ~15, ~9, and ~7 meV [see Figs. 2(b)–2(i)]. We then searched for the RW's by plotting the eigendisplacements of atoms in the layers adjacent to the surface layer for eigenmodes in these regions. We were able to identify a few distinctive RW's. Among them are one mode at 12.7 meV (mostly *z* polarized), one at 8.3 meV (mostly *xy* polarized), and one at 7.2 meV (mostly *z* polarized), in good agreement with the experimental result of Ref. 2. These modes were found to have a decay length of the order of 1–2 nm along the *z* direction.

In conclusion, our NOTB-MD studies of a semi-infinite Si(111)-7×7 surface have revealed RW modes, a low-energy mode (16 meV) associated with the stacking fault with its peak at the rest atom in the faulted half, a mode (57 meV) localized within the first two layers, two modes that are narrowly separated in energies (nearly degenerate) but with distinct features (62–63 meV), and a split-off mode above the bulk spectrum. The new modes uncovered in the present work, but not reported in the previous studies,[4–6] suggest that surface dynamical features are sensitive to the system size and structural relaxations. Further confirmations of our findings by experiments are necessary.

This work was supported jointly by the NSF (Contract No. DMR-011284) and the U.S. DOE (Contract No. DE-FG02-00ER45832).

[1] W. Daum, H. Ibach, and J.E. Muller, Phys. Rev. Lett. **59**, 1593 (1987).

[2] G. Lange, J.P. Toennies, P. Ruggerone, and G. Benedek, Europhys. Lett. **41**, 647 (1998).

[3] X.-P. Li, G. Chen, P.B. Allen, and J.Q. Broughton, Phys. Rev. B **38**, 3331 (1988).

[4] J. Kim, M.-L. Yeh, F.S. Khan, and J.W. Wilkins, Phys. Rev. B **52**, 14 709 (1995).

[5] I. Stich, K. Terakura, and B.E. Larson, Phys. Rev. Lett. **74**, 4491 (1995).

[6] I. Stich, J. Kohanoff, and K. Terakura, Phys. Rev. B **54**, 2642 (1996).

[7] M. Menon and K.R. Subbaswamy, Phys. Rev. B **55**, 9231 (1997).

[8] S. Liu, C.S. Jayanthi, S.Y. Wu, X. Qin, Z. Zhang, and M.G. Lagally, Phys. Rev. B **61**, 4421 (2000).

[9] I. Stich, M.C. Payne, R.D. King-Smith, J.S. Lin, and L.J. Clarke, Phys. Rev. Lett. **68**, 1351 (1992).

[10] We have substantiated our claim by carrying out a relaxation under the same condition used in Refs. 4,9. We found the distance between the adatom and the layer-2 atom directly underneath it to be 2.6 Å, in agreement with the TB result of Ref. 4. Furthermore, calculation in Ref. 8 indicated that the inclusion of an *ad hoc* Hubbard-like term, although moderates the charge transfer in the buckled dimers of the reconstructed Si(001) surface, changes the surface energy by only less than 0.01 eV/atom, inducing no significant change in the structure. Considering that no unusual configuration such as the buckled dimers on the surface of the Si(111)-7×7 surface, it is even more unlikely that there will be any appreciable effect on the dynamics of the Si(111)-7×7 surface associated with the charge transfer.

[11] See, for example, S.Y. Wu and C.S. Jayanthi, Int. J. Mod. Phys. B **9**, 1869 (1995), and references therein.

[12] W. Weber, Phys. Rev. B **15**, 4789 (1977).

[13] L. Liu, C.S. Jayanthi, and S.Y. Wu, Phys. Rev. B **68**, 012303 (2003).